NASA TECHNICAL NOTE

A FORMAL STRUCTURE FOR ADVANCED AUTOMATIC FLIGHT-CONTROL SYSTEMS

George Meyer and Luigi Cicolani

Ames Research Center
Moffett Field, Calif. 94035

NATIONAL AERONAUTICS AND SPACE ADMINISTRATION • WASHINGTON, D. C. • MAY 1975

1. Report No.	2. Government Accession No.
TN D-7940	

4. Title and Subtitle
A FORMAL STRUCTURE FOR ADVANCED AUTOMATIC FLIGHT-CONTROL SYSTEMS

5. Report Date
May 1975

6. Performing Organization Code

7. Author(s)
George Meyer and Luigi Cicolani

8. Performing Organization Report No.
A-5710

10. Work Unit No.
501-03-11

9. Performing Organization Name and Address
Ames Research Center
Moffett Field, Calif., 94035

11. Contract or Grant No.

13. Type of Report and Period Covered
Technical Note

12. Sponsoring Agency Name and Address
National Aeronautics and Space Administration
Washington, D. C. 20546

14. Sponsoring Agency Code

15. Supplementary Notes

16. Abstract

An effort is underway at Ames Research Center to develop techniques for the unified design of multimode, variable authority automatic flight-control systems for powered-lift STOL and VTOL aircraft. This report describes a structure for such systems which has been developed to deal with the strong nonlinearities inherent in this class of aircraft, to admit automatic coupling with advanced air traffic control requiring accurate execution of complex trajectories, and to admit a variety of active control tasks. The specific case being considered is the augmentor wing jet STOL research aircraft.

17. Key Words (Suggested by Author(s))
Handling qualities
Flight controls
Autopilot

18. Distribution Statement
Unclassified - unlimited

STAR Category - 08

19. Security Classif. (of this report)	20. Security Classif. (of this page)	21. No. of Pages	22. Price*
Unclassified	Unclassified	39	$3.75

*For sale by the National Technical Information Service, Springfield, Virginia 22151

TABLE OF CONTENTS

SYMBOLS

A_{as}	direction cosine matrix, actual attitude of the aircraft with respect to inertial space
A_{cs}	direction cosine matrix, commanded attitude of the aircraft with respect to inertial space
A_{vs}	direction cosine matrix, commanded velocity axes with respect to inertial space
b	wing span
c	wing chord
C_D	drag coefficient
C_{Dc}	commanded drag coefficient
C_J	cold thrust coefficient
C_L	lift coefficient
C_{Lc}	commanded lift coefficient
C_{Ma}	moment coefficient vector with respect to body axes
C_{Mac}	commanded moment coefficient with respect to body axes
C_s	total force vector coefficient
D	drag
$E_i(\phi)$	elementary rotation about axis i through angle ϕ
f_s	total aerodynamic and propulsive force in inertial coordinates
$f(x,u)$	right-hand side of system state equation
g	acceleration of gravity
$g(\dot{x},x)$	trimmap
h_a	body coordinates of total angular momentum
$h(e)$	right-hand side of transition dynamics
$K(\dot{x},x)$	feedback gain schedule
L	lift

m	aircraft mass
M_a	body coordinates of aerodynamic and propulsive moment
Q	dynamic pressure
R_s	inertial coordinates of position vector
R_s^*	inertial coordinates of position vector commanded by air traffic control
R_{sc}	inertial coordinates of position given by command generator
S_w	wing area
t	time variable
δT	throttle
T_c	cold thrust
T_h	hot thrust
u	control vector
u_a	body coordinates of unit vector along relative velocity vector
u_s	inertial coordinates of unit vector along relative velocity vector
v	airspeed (true airspeed)
v_a	body coordinates of relative velocity vector
v_{am}	measured body coordinates of relative velocity vector
v_s	inertial coordinates of relative velocity vector
V_s	inertial coordinates of aircraft velocity vector
V_s^*	inertial coordinates of velocity commanded by air traffic control
V_{sc}	inertial coordinates of velocity commanded by command generator
$\dot{V}_s$	inertial coordinates of aircraft acceleration vector
$\dot{V}_s^*$	inertial coordinates of acceleration commanded by air traffic control
$\dot{V}_{sc}$	inertial coordinates of acceleration commanded by command generator
$\dot{V}_{sI}$	inertial coordinates of acceleration input to trimmap

$\dot{V}_{sm}$	inertial coordinates of acceleration modifications due to perturbation controller
w_s	inertial coordinates of wind
$\hat{w}_s$	inertial coordinates of estimated wind
x	system state
α	angle of attack
β	angle of sideslip
γ_v	glide-slope angle of relative velocity vector
δ_{ec}	elevator command
δ_F	flap angle
δ_i	column matrix with 1 in ith row and 0 in the other two rows
δ_{rc}	rudder command
δ_T	throttle command
δ_{wc}	wheel command
η	variables of unsteady aerodynamics
θ	pitch angle
ν	nozzle angle
ρ	density of air
σ	side-force angle
ϕ	roll angle
ψ	yaw angle
ω_a	body coordinates of aircraft angular velocity
ω_n	bandwidth

A FORMAL STRUCTURE FOR ADVANCED AUTOMATIC FLIGHT-CONTROL SYSTEMS

George Meyer and Luigi Cicolani

Ames Research Center

SUMMARY

An effort is underway at Ames Research Center to develop techniques for the unified design of multimode, variable authority automatic flight-control systems for powered-lift STOL and VTOL aircraft. This report describes a structure for such systems which has been developed to deal with the strong nonlinearities inherent in this class of aircraft, to admit automatic coupling with advanced air traffic control requiring accurate execution of complex trajectories, and to admit a variety of active control tasks. The specific case being considered is the augmentor wing jet STOL research aircraft.

INTRODUCTION

Government and industry are investing substantial resources in developing new aircraft configurations required to meet the needs of the nation in the 1980's and beyond. Present indications are that automatic flight-control systems will play a significant role in this development. The basis for such a forecast is a combination of three factors.

1. The mix of aircraft types such as VTOL, STOL, CTOL, and SST will require an advanced air traffic control (ATC) system. The accommodation of many aircraft covering a wide spectrum of speeds and maneuverability and at the same time satisfying stringent environmental constraints can be achieved only if the ATC has at its disposal a sufficiently large set of trajectories. Accurate execution of any one of a large set of complex trajectories will require a powerful automatic flight-control system that uses the maximum capability of each aircraft type.

2. Current work aimed at providing aircraft for short-haul transportation is developing the powered-lift technology. Among the concepts being considered are the augmentor wing, tilt rotor, lift fan, and externally blown flap. In all cases, the wide range of lift coefficient is achieved by inflight modifications of the aircraft configuration.

These modifications result in drastic changes in control characteristics of the aircraft; particularly in the high lift transition and landing configurations, the aircraft response to control inputs is very nonlinear. Moreover, the presence of powered- and direct-lift generators increases the total number of controls available to the pilot who must continually make decisions

on control techniques. Accurate, unaided manual tracking of complex trajectories by manipulating a large set of interacting controls of an aircraft whose control characteristics are nonlinear and rapidly changing represents an unacceptably high pilot workload. Automatic flight control can reduce the pilot workload to an acceptable level by integrating control functions so as to generate desirable handling qualities without reducing the performance of the aircraft as an element of the advanced civil air transportation system. The advantages of automatic flight control are potentially even more substantial in military applications of STOL and VTOL aircraft. Both the advanced military STOL and the Sea Control Fighter VTOL must utilize to the fullest the maneuvering capability of the basic aircraft. The tracking of complex trajectories must be sufficiently accurate to properly execute a mission, and the pilot workload associated with flying must not adversely affect his ability to perform other tasks. Again, the maneuverability, accuracy, flexibility, and level of pilot workload can be improved with automatic flight control.

3. The rapidly advancing technology of sensors, actuators, and electronic components is approaching the point when servomechanisms with reliability comparable to that of a wing can be built and maintained economically. Consequently, the conventional direct mechanical systems composed of cables, push rods, bell cranks, and mixers that link the pilot to control surfaces can be replaced by fly-by-wire systems. Although fly-by-wire technology itself offers several advantages over the conventional mechanical control systems, the real goal lies in the application of active control technology (ACT) to future aircraft. The key idea of ACT is the integration of control with aerodynamics, structures, and propulsion early in the design cycle of the aircraft. Studies have shown that significant reductions in induced drag and structural weight, improvements in passenger comfort, and reduction of flight hazards can be achieved with ACT. These benefits are possible due to (a) a reduction in the sizes of stabilizing surfaces, with stability provided by dynamically controlling movable surfaces rather than statically with larged fixed surfaces as in the conventional designs; (b) reductions in structural strength requirements by applying maneuver load alleviation and gust load alleviation; (c) improvement of ride qualities by a ride quality control system; and (d) reduction in the occurrence of inadvertent flight hazard through automatic limitation of flight conditions. These and other ACT concepts are currently being developed. A total automatic flight-control system is required to integrate all these control functions with the autopilot.

Thus, indications are that automatic flight-control systems will play a significant role in the development of future aircraft. Of course, these systems were needed in the past, but the designer was severely limited by the characteristics of available transducers and, particularly, by the small inflight computational capacity. However, rapid advances have resulted in a large variety of accurate and reliable devices, while the capacity of digital flight computers has increased phenomenally and continues to increase. As a result, the designer is now limited primarily by the available methodology for the design of automatic flight-control systems.

The most severe limitation of the existing design techniques is their extreme reliance on linear perturbation models of the aircraft. So long as

nonlinear effects are of minor significance, these techniques are quite adequate. But as nonlinearities become prominent because of either increased system accuracy requirements or the physics of force and moment generation in the powered-lift configurations, linear methods become less tractable. Many perturbation models are needed to cover the flight envelope adequately. Even the procedure for choosing reference trajectories about which to perturb is unclear at present, and controls corresponding to these trajectories that trim the aircraft cannot be generated easily or accurately by means of perturbation techniques. Logic must be provided in the flight computer for switching the perturbation control gains and reference controls as the aircraft leaves the domain of validity of one perturbation model and enters another. The result is a design that is complex in concept and implementation so that analyses of closed-loop sensitivity to modeling errors and subsystem failures are exceedingly difficult and not very convincing.

Design techniques are needed of sufficient generality to be applicable to a large set of aircraft types with nonlinear dynamics and multiple redundant controls. The techniques must admit an effective tradeoff between tracking accuracy requirements on the one hand and requirements imposed on the capacity of the flight computer and on the a priori knowledge of system dynamics on the other hand. The techniques must be nearly algorithmic to permit tradeoff studies early in the aircraft design cycle when many alternative aircraft configurations are being considered. Techniques are needed for integrating a variety of active control functions with an autopilot having a multitude of modes and for coupling the autopilot automatically with the air traffic control. Finally, these design techniques must result in designs sufficiently simple to admit an effective reliability analysis.

An effort is underway at Ames to develop the methodology for the design of advanced flight-control systems. This report describes the progress made in the first segment of this program, namely, the formulation of an overall logical structure for multimode, variable authority, automatic flight-control systems. The proposed structure consists of five major subsystems: (1) The force trimmap trims the aircraft to any admissible time-varying acceleration vector. One of the outputs of the force trimmap is the possibly time-varying trim attitude. (2) The attitude control system generates commands to the moment-generating control surfaces and thereby forces the aircraft attitude to follow the input from the force trimmap. (3) The wind estimator provides estimates of the aircraft velocity vector relative to the air mass which are needed in the force trimmap and attitude control system calculations. (4) The trajectory perturbation controller closes the loop around the inaccuracies of the force trimmap, attitude control system, and wind estimator. The result is a trajectory acceleration vector controller whose input-output relation between the commanded acceleration and actual aircraft acceleration is essentially an identity, provided the input is flyable and its bandwidth is suitably restricted. (5) The trajectory command generator transforms the inputs from the air traffic control or the pilot into trajectories whose acceleration is consistent with the limitations of the trajectory acceleration controller. The basis for the proposed structure as well as its feasibility, benefits, and limitations are discussed. The internal structure of the five major subsystems is presented in some detail to clarify the intent of each subsystem.

The augmentor wing jet STOL research aircraft is used as a specific example. It is emphasized, however, that the objective of this report is not to present a complete automatic flight-control system for a particular aircraft, but rather to propose an overall logical structure for such systems.

BASIC COMMANDS TO AUTOMATIC FLIGHT-CONTROL SYSTEM

The boundary of the system considered here is shown schematically in figure 1. In the following discussion, the automatic flight-control system is the complete control system of the aircraft. It consists of all sensors, actuators, and control logic. The set of sensors measures aircraft motion and includes devices that are onboard as well as ground-based systems such as the MLS (when available). The function of the control logic is to operate on the data from the sensors and commands from the (generalized) air traffic control (ATC) and thereby to generate commands to the actuators which, in turn, control the aircraft. The degree of automation of the control logic ranges from the fully automatic mode, in which the actuators are completely under the control of the flight computer, to the fully manual mode, in which the actuators are controlled exclusively by the pilot. Between these extremes, there is a spectrum of modes with specific functions such as handling quality control, ride quality control, gust load alleviation, maneuver load control, and a variety of autopilot modes such as autothrottle, altitude hold, heading capture, etc. Of course, combinations of such elementary modes may also be required. In addition, the control logic must be able to detect failures in various subsystems and switch (when necessary) to the next safest control strategy. The subject of this report is the design of such control logic. (The estimation problem associated with sensors and the design of fly-by-wire systems is not discussed.)

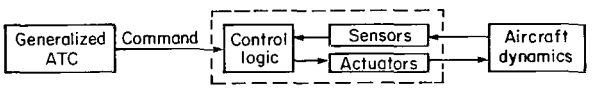

Figure 1.- Elements of automatic flight control system.

The basic input to the control logic is the trajectory to be followed by the aircraft. The trajectory may be commanded explicitly by the ATC or implicitly by the pilot. A simple case, conceptually, occurs when (based on wind estimates, the capabilities of the aircraft, and other considerations) ATC selects a flyable trajectory to be followed by the aircraft. Generally, the set of admissible trajectories consists of a sequence of continuous segments defined on relatively long (e.g., greater than 10 sec) intervals of time (ref. 1). Often the segments belong to a small set (e.g., lines and circles), in which case only the parameters and duration of the segments are transmitted to the aircraft and the commanded trajectory is reconstructed onboard. Otherwise, the coordinates of the trajectory are transmitted to the aircraft continuously. In either case, the segments are defined on intervals of time; hence, position, velocity, and acceleration vectors corresponding to the commanded trajectory are available to the control logic continuously. Moreover, since the motion of the aircraft in inertial space (a flat nonrotating earth is assumed throughout for simplicity) is of prime concern, inertial

coordinates of these vectors are considered as fundamental. The situation is essentially the same whenever the aircraft is commanded to coincide with a moving target as, for example, a carrier landing or docking with another aircraft or a missile intercepting another object.

The pilot is an alternative source of commands. Of course, if he feeds the trajectory parameters into the autopilot either as a voice command from ATC or on his own initiative, he may be considered part of the ATC. However, many of the commonly used autopilot modes such as heading hold, altitude hold, autothrottle, glide-slope capture, control wheel steering, etc., generate the commanded trajectory only implicitly and often incompletely. Nevertheless, in most cases, an appropriate equivalent ATC trajectory can be constructed to represent the pilot command. The trajectory may contain a number of free parameters which the control logic can be instructed to ignore. Consequently, most commands concerning the motion of the aircraft center of mass may be considered, at least conceptually if not in actual mechanization, to be generated in a standard form by the generalized ATC.

In view of the preceding discussion, the following decision is made concerning the structure of the automatic flight-control system:

Decision 1: The basic command to the automatic flight-control system is a concatenation of continuous segments Γ_k^*, each of which is given by

$$\Gamma_k^* = \left\{ y^*(t) = \begin{pmatrix} R_s^*(t) \\ V_s^*(t) \\ \dot{V}_s^*(t) \end{pmatrix}, \quad t \in T_k^* \right\}, \quad k = 1,2,\ldots \tag{1}$$

where the 9-tuple consists of inertial coordinates of commanded inertial position (R_s^*), velocity (V_s^*), and acceleration ($\dot{V}_s^*$) vectors.

The complete trajectory may have discontinuities across the boundaries of the intervals T_k. For example, all coordinates are discontinuous at $t = t_4$ in figure 2. The control logic must synthesize a transition trajectory consistent with the limitations imposed by dynamics. Another possibility is

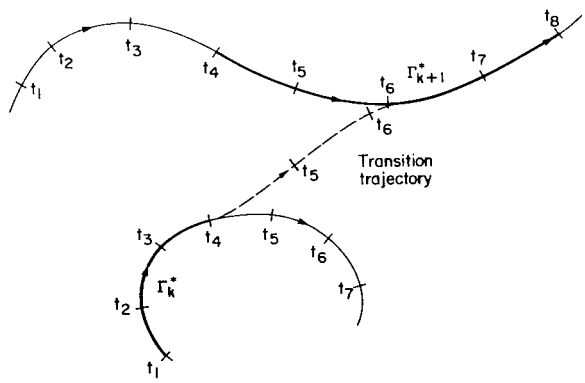

Figure 2.- A trajectory $\Gamma^* = \ldots \Gamma_k^* \Gamma_{k+1}^* \ldots$ with total discontinuity at $t = t_4$.

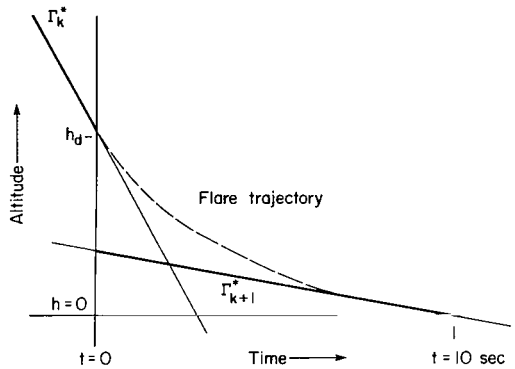

Figure 3.- ATC command, $\Gamma^* = \ldots \Gamma_{k+1}^*$, to land.

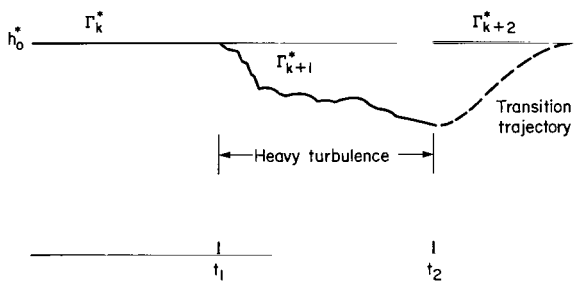

Figure 4.- Encounter with heavy turbulence.

illustrated in figure 3, which represents the vertical channel of the command to land. The segment Γ_k^* correspond to altitude variation while the aircraft is on the glide slope. The flare initiation altitude occurs at $t = 0$, at which time the segment Γ_{k+1}^* is commanded. Thus there is a discontinuity in both position and velocity at $t = 0$. Again, the control logic must synthesize an appropriate transition (flare) trajectory.

As already noted, some parameters of the commanded trajectory may be free. In particular, all nine coordinates need not be always tracked. For example, consider the three segments shown in figure 4. Segment Γ_k^* represents the command to track a four-dimensional trajectory with constant altitude h_o^*. At $t = t_1$, the aircraft encounters heavy turbulence. Depending on the severity of the turbulence relative to the limits imposed on aircraft dynamics, tracking may have to be relaxed from position, to velocity, or acceleration and, in the extreme case, only the attitude of the aircraft will be tracked while the ATC command is ignored completely. As a result, the aircraft is allowed to drift along some trajectory Γ_{k+1}^* away from the true ATC command. As turbulence subsides at $t = t_2$, four-dimensional tracking can be resumed. However, because of the errors accumulated in the interval (t_1, t_2), there will be, in general, a discontinuity in all coordinates of the command at $t = t_2$. The control logic must synthesize an appropriate transition trajectory to bring the aircraft back on Γ_{k+2}^*. The situation is essentially the same when the set of operating sensors changes with time or when the constraints imposed on the aircraft dynamics change perhaps because of failures in certain subsystems.

Based on the preceding discussion, the following decision is made concerning the formal structure of the control system.

Decision 2: The control logic contains a command generator that synthesizes trajectories

$$\Gamma = \left\{ y(t) = \begin{pmatrix} R_{sc}(t) \\ V_{sc}(t) \\ \dot{V}_{sc}(t) \end{pmatrix} , \forall t \right\}$$

which are flyable at all times by the aircraft with the available sensors and actuators and with existing constraints imposed on dynamics.

For example, the output of the command generator corresponding to the case in figure 3 is shown in figure 5. Note that there is no discontinuity in Γ at $t = 0$; while there is a discontinuity in Γ^* at the same instant. (The command generator is discussed further later in the report.)

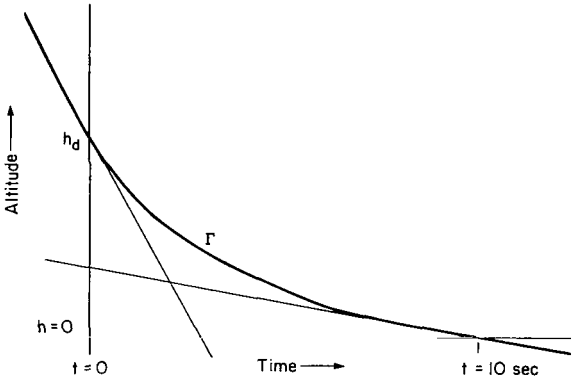

Figure 5.- Output of the command generator for a landing maneuver.

TRACKING ACCURACY

Clearly, one of the essential attributes of a control system is that it be as simple as possible, both in concept and in mechanization. The level of complexity, however, is determined ultimately by accuracy requirements. If the required accuracy is low, then many details of the aircraft equation of motion may be suppressed, and a simple model usually leads to a simple control law. As accuracy requirements are increased, a more detailed representation of aircraft dynamics becomes necessary. The model increases in complexity. The dimension of its state space increases as more dynamical elements are accounted for. New cross-coupling links appear. The number of parameters increases with finer representation of nonlinearities. All this increases the complexity of the control system. Moreover, the design methodology may have to be changed completely with an increase in accuracy requirement. As a result, tradeoff studies may become intractable. However, such studies are essential in the design of automatic flight-control systems advanced aircraft. Of particular interest is the tradeoff between the required capacity of the onboard computer and trajectory tracking accuracy. Hence, a single design methodology must be developed in which tracking accuracy is a variable.

The natural evolution of an AFCS for a new, possibly experimental, aircraft is by means of a sequence of refinements. For safety, initial flight tests are restricted to relatively simple maneuvers and to correspondingly simple modes of the control system with minimal authority and tracking accuracy. As flight data accumulate and good estimates of critical aircraft parameters become available, the set of maneuvers is expanded until, finally, it coincides with the designed flight envelope. Thus, the automatic flight-control system must be designed to allow a spectrum of tracking and modeling accuracies.

A spectrum of accuracy, rather than a single level, is also needed for normal aircraft operation. For example, in cruise, altitude tracking is

obviously not as significant as during a landing maneuver and can be traded for, say, ride quality.

Therefore, the following decision is made concerning the structure of the control system.

Decision 3: The tracking accuracy enters the control logic as an independent variable, both during design as well as in normal operation.

The accuracy of a control system is ultimately limited by the accuracy of the navigation system. Hence the accuracy of the latter serves as an estimate of an upper bound on the former. The RAINPAL system (ref. 2) is one of the most accurate, flight-tested, navigation systems currently available. A comparison of RAINPAL errors with allowable errors for CTOL and SSV is given in table 1. In the remainder of this report, the RAINPAL errors are taken as the upper limit on the trajectory tracking requirements.

TABLE 1.- COMPARISON OF RAINPAL NAVIGATION ERRORS WITH ALLOWABLE ERRORS FOR CTOL AND SSV

Component	RAINPAL navigation error standard deviations	Navigation errors allowable for CTOL automatic landing systems	Navigation errors allowable for the SSV autoland system
X	0.9 ±0.6 m (3 ±2 ft)	132 m (433 ft)	43.2 m (139 ft)
Y	1.2 ±0.6 m (4 ±2 ft)	2.38 m (7.79 ft)	1.51 m (4.97 ft)
Z	0.9 ±0.6 m (3 ±2 ft)		2.46 m (8.08 ft)
$\dot{X}$	0.15 ±0.06 m/sec (0.5 ±0.2 ft/sec)		1.76 m/sec (5.77 ft/sec)
$\dot{Y}$	0.3 ±0.15 m/sec (1 ±0.5 ft/sec)		0.88 m/sec (2.89 ft/sec)
$\dot{Z}$	0.15 ±0.06 m/sec (0.5 ±0.2 ft/sec)		0.088 m/sec (0.289 ft/sec)

EQUATIONS OF MOTION

Let the inertial coordinates of the aircraft position and velocity with respect to the runway axes (flat, nonrotating earth is assumed throughout) be denoted by R_s and V_s, respectively. Then

$$\dot{R}_s = V_s \tag{3}$$

where $(\dot{})$ denotes differentiation with respect to time t. Aerodynamic forces and moments depend on the velocity of the aircraft relative to the air mass. Let W_s denote the inertial coordinates of the wind velocity. Generally, W_s is a complicated function of position and time which may vary significantly over the dimensions of the aircraft. Let

$$W_s = w_s(R_s,t) + \delta w_s(R_s + r_s,t) \tag{4}$$

where the first and second terms consist of wavelengths longer and shorter, respectively, than the aircraft dimensions, and r_s is position-referenced to the aircraft center of mass. The inertial coordinates v_s of the aircraft velocity relative to the air mass are defined in this report by

$$v_s = V_s - w_s \tag{5}$$

where $w_s = w_s(R_s,t)$ is the average wind at the aircraft center of mass. Wind shear across the aircraft is ignored here. Polar coordinates of relative velocity are defined in a standard manner according to figure 6. Thus

$$v_s = vu_s \tag{6}$$

and

$$u_s = E_3^T(\psi_v)E_2^T(\gamma_v)\delta_1 \tag{7}$$

where $E_i(\phi)$ is an Euler rotation about axis i, $(\ )^T$ is the transpose of $(\ )$, and δ_i is the column with 1 in the ith place and 0 in the other two. In the absence of wind, ψ_v is the aircraft heading angle and γ_v is the glide-slope angle.

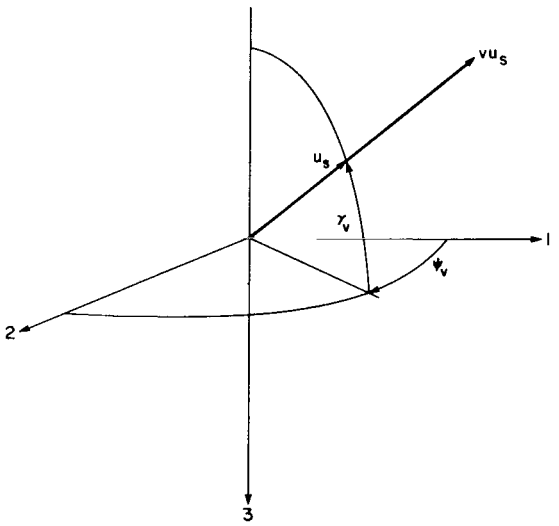

Figure 6.- Definition of airspeed, v, heading angle ψ_v and glide slope angle γ_v.

In the aircraft body axes, the relative velocity is given by

$$v_a = vu_a \tag{8}$$

where

$$u_a = E_2(\alpha)E_3^T(\beta)\delta_1 \tag{9}$$

Conversely,

$$\left.\begin{aligned} \alpha &= \tan^{-1}[u_a(3)/u_a(1)] \\ \beta &= \sin^{-1}[u_a(2)] \end{aligned}\right\} \tag{10}$$

where α and β are the angle of attack and sideslip angle as normally defined (ref. 3).

The attitude of the aircraft body axes with respect to the runway axes are defined by the direction cosine matrix A_{as}. If Euler angles are used in the 3-2-1 sequence, then

$$A_{as} = E_1(\phi)E_2(\theta)E_3(\psi) \tag{11}$$

The attitude can also be defined in terms of the angles associated with the direction of the relative velocity vector as

$$A_{as} = E_2(\alpha)E_3^T(\beta)E_1(\phi_v)E_2(\gamma_v)E_3(\psi_v) \tag{12}$$

where ϕ_v is the angle of roll about the relative velocity vector v_s. A block diagram representation of equation (12) is given in figure 7 for future reference. The term "heading" refers to the heading of the relative velocity vector.

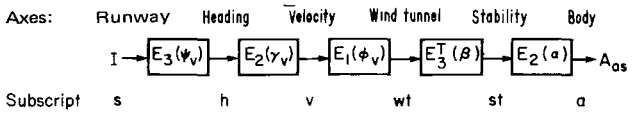

Figure 7.- Block diagram representation of equation (13).

Let the body coordinates of aircraft angular velocity with respect to the runway be denoted by ω_a. Then (see, e.g., ref. 4),

$$\dot{A}_{as} = S(\omega_a)A_{as} \tag{13}$$

where, for any column $x = (x_1, x_2, x_3)^T$,

$$S(x) = \begin{pmatrix} 0 & x_3 & -x_2 \\ -x_3 & 0 & x_1 \\ x_2 & -x_1 & 0 \end{pmatrix} \tag{14}$$

Equations (3) and (13) are the kinematic components of the aircraft equations of motion.

Let the inertial coordinates of total aerodynamic and propulsive force be denoted by f_s, and let m and g be the aircraft mass and acceleration of gravity, respectively. Then

$$\dot{V}_s = \frac{1}{m} f_s + g\delta_3 \tag{15}$$

The total aerodynamic and propulsive force is most directly expressed in terms of coordinates with respect to the wind-tunnel axes. Thus the total force along the relative velocity vector, henceforth to be called total drag,

$$D_{wt} = -QS_w C_D \delta_1 \tag{16}$$

where the dynamic pressure

$$Q = \frac{1}{2} \rho v^2 \tag{17}$$

for which ρ is the density of air, S_w is the wing area, and C_D is the total drag coefficient. The total force perpendicular to the relative velocity vector, henceforth to be called total lift,

$$L_{wt} = -QS_w C_L E_1^T(\sigma)\delta_3 \tag{18}$$

where C_L is the total lift coefficient and σ is defined in figure 8. Note that the present definition of the total lift coefficient includes the side force, and both total lift and drag coefficients include the effects of thrust. Generally,

$$\left.\begin{aligned} C_D &= C_D(\alpha,\beta,u;\eta) \\ C_L &= C_L(\alpha,\beta,u;\eta) \\ \sigma &= \sigma(\alpha,\beta,u;\eta) \end{aligned}\right\} \tag{19}$$

where u represents the available controls such as flaps, throttle, elevator, rudder, ailerons, etc., and η represents the dynamic variables such as α, $\dot{\beta}$, ω_a, etc., and other variables such as air temperature and density.

The inertial coordinates of the total aerodynamic and propulsive force are given by

$$f_s = QS_w C_s \tag{20}$$

where the total force vector coefficient is

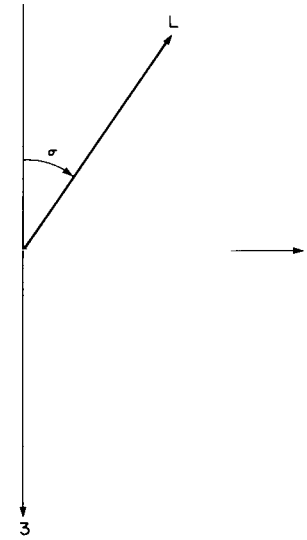

Figure 8.- Definition of lift vector used in report.

$$C_s = -A_{as}^T E_2(\alpha) E_3^T(\beta) [C_D \delta_1 + C_L E_1^T(\sigma) \delta_3] \tag{21}$$

The dynamic equation for rotation is given by

$$\dot{\omega}_a = J_a^{-1} [M_a + S(\omega_a) h_a] \tag{22}$$

where J_a is the aircraft moment of inertia in body axes, M_a is the total aerodynamic and propulsive moment, and h_a is the total aircraft angular momentum. When the angular momentum of spinning parts is negligible,

$$h_a = J_a \omega_a \tag{23}$$

The moment vector is defined in terms of the moment coefficients in the usual manner:

$$M_a = QS_w \begin{pmatrix} b & 0 & 0 \\ 0 & c & 0 \\ 0 & 0 & b \end{pmatrix} C_{Ma} \tag{24}$$

where b and c are the span and mean chord, respectively, of the wing. Generally,

$$C_{Ma} = C_m(\alpha, \beta, u; \eta) \tag{25}$$

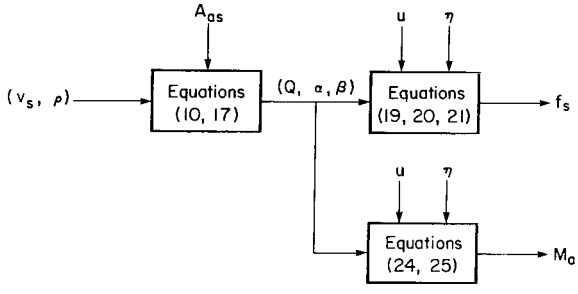

Figure 9.- Main information flow in force and moment generation.

The data represented by equations (19) and (25) are considered as the fundamental source of information concerning the total aerodynamic and propulsive force and moment. In the remainder of this report, these data are assumed to be given to various levels of accuracy. The information flow involved in force and moment generation is shown in figure 9.

Equations (3), (13), (15), and (22) are the fundamental components of the system state equation. Other effects such as the dynamics of actuators and sensors may be adjoined to these equations as the need arises to obtain the complete state equation modeling the aircraft.

AUGMENTOR WING JET STOL RESEARCH AIRCRAFT

A specific aircraft is described here to motivate and aid in the following discussion. Note that, although the discussion in the remainder of the report is directed toward this specific aircraft, the essential concepts are applicable to other types of aircraft.

The augmentor wing jet STOL research aircraft (AWJSRA) is a de Havilland C-8A "Buffalo" modified according to the general arrangement shown in figure 10. The wing area S_w is 80.36 m^2 (865 ft^2) and the maximum gross weight is 20,400 kg (45,000 lb). The aircraft is powered by two turbofan engines. The relatively cold flow from the front fans is ducted through the wing and fuselage to the augmented jet flap and blown ailerons. The arrangement of the augmentor flap is shown in figure 11. The entire flap unit pivots about the main hinge point. No provision is made in this installation to retract the upper flap units into the main wing contour. The Coanda surface serves to deflect the (cold) flow from the nozzle. The augmentor chokes at the trailing edges of the main flaps control the lift generated by the flaps. The two outboard flap chokes are used to control roll and all four chokes are used to spoil lift after landing.

The hot gas from the two turbofan engines flows through two pairs of nozzles that can be rotated in flight to provide vectoring of the hot thrust through a range of 98°. All nozzles are connected to move in unison in response to a single nozzle angle command. The geometry associated with the hot thrust is shown

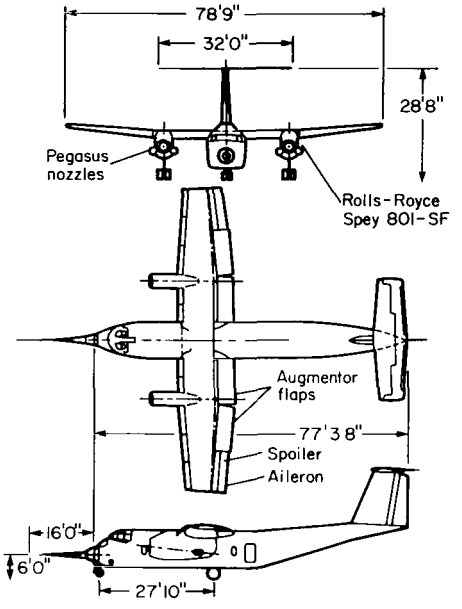

Figure 10.- General arrangement of the modified C-8A.

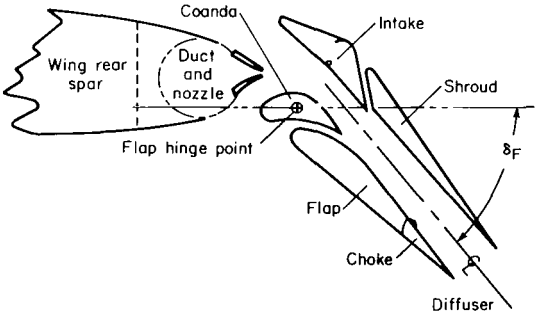

Figure 11.- Arrangement of the augmentor flap.

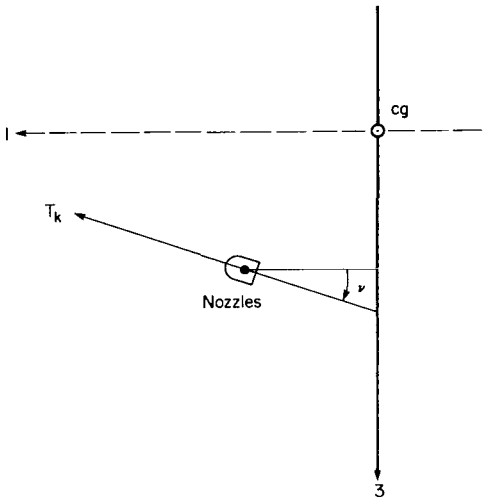

Figure 12.- Geometry of hot thrust in body coordinates.

in figure 12. Since the aircraft center of gravity is not on the axis of rotation of the nozzles, the hot thrust generates a moment that depends on the nozzle angle ν. The servos that control the nozzles are quite fast, being limited to 90°/sec. The hot and cold thrusts depend on the engine speed. The speed of both engines is controlled in unison by a single throttle command, δ_T. The associated servo system is relatively slow with a bandwidth of approximately 1 rad/sec. The cold flow has a pronounced effect on the wing-body polars of the aircraft as shown in figure 13, where the independent variables are flap angle δ_F, angle of attack α, and cold thrust coefficient $C_J = T_c/QS_w$.

Of particular significance for the design of automatic trajectory tracking systems is the large variation in the basic aerodynamic characteristics of the aircraft (evident in fig. 13). Certainly, there is quite a significant change between cruise configuration (flap = 4.5°) and landing configuration (flap = 65°). But present indications are that the nonlinearity is significant even over much smaller regions. For example,

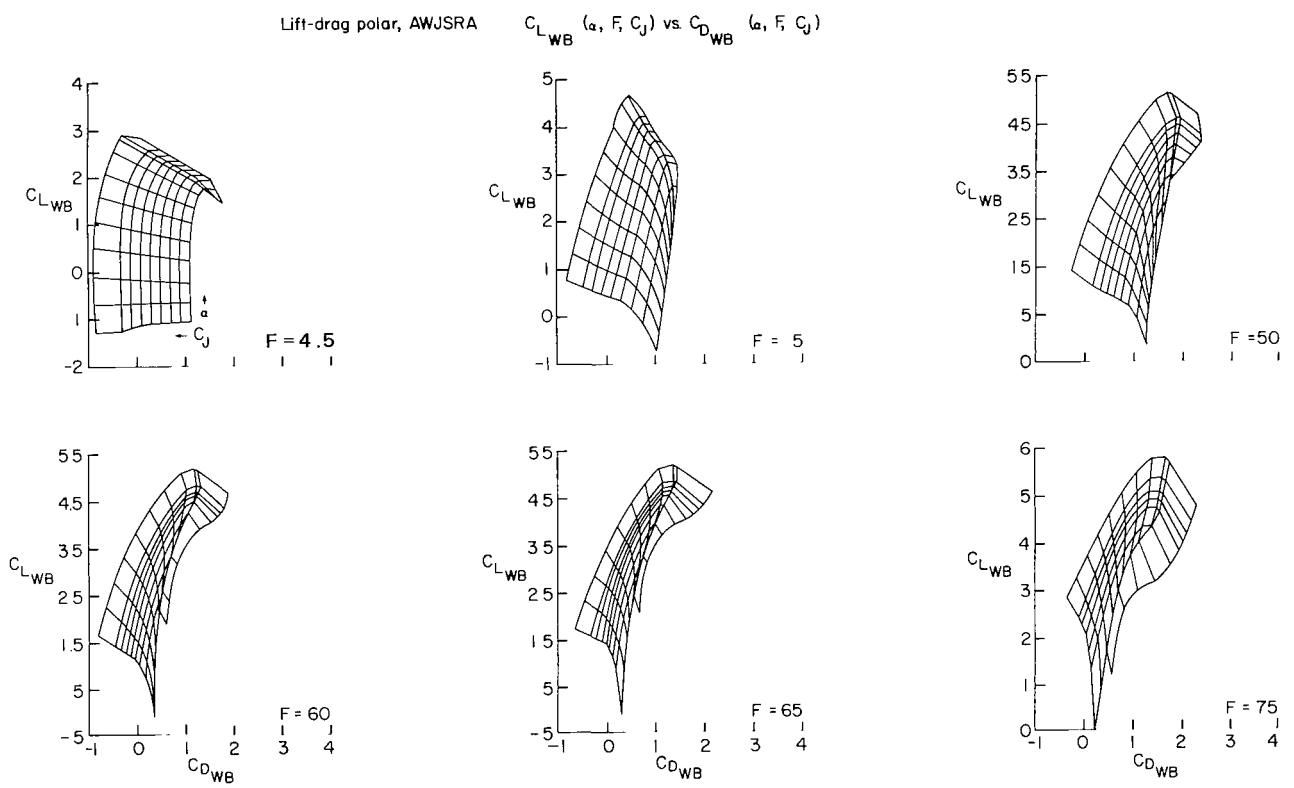

Figure 13.- Wing-body polars $(C_D, C_L)(\alpha, C_J, \delta_F)$.

figure 14 shows the total lift and drag coefficients, including the effects of the hot thrust for a constant flap, throttle, and airspeed which correspond to a typical landing configuration with angle of attack and nozzle angle as the independent variables.

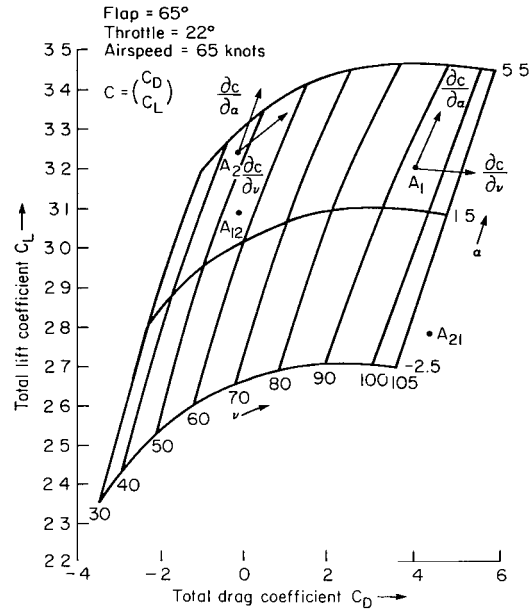

Figure 14.- Total force coefficient.

Point A_1 represents equilibrium flight at 65 knots along the -7.5° glide slope. Point A_2 represents level flight at the same speed. The derivatives of the total force vector coefficients are also shown at these two points. As the aircraft is maneuvered between A_1 and A_2, the change in these derivatives may adversely affect closed-loop stability. Of additional concern is the magnitude of steady-state error in altitude which will result if linearity is assumed in this region. Thus, for a maneuver that takes the aircraft from A_1 to A_2, the feedforward based on the linear model at A_1 will trim the aircraft to point A_{12} giving an error in the required lift coefficient, $\Delta C_L/C_L$ = 4.5 percent. This error will be absorbed by the altitude feedback, resulting in an error $h_e = 0.045g/\omega_n^2$, where g is the acceleration of gravity and ω_n is the bandwidth of the altitude loop. But, because of limitations imposed by the unsteady aerodynamics on this bandwidth, $\omega_n \leq 0.5$ rad/sec at 65 knots; hence $h_e \geq 1.8$ m (5.8 ft). Similarly, a maneuver that takes the aircraft from level flight (point A_2) onto the -7.5° glide slope (point A_1) by means of the feedforward based on the linear model at A_2 will be trimmed to point A_{21}, resulting in a magnitude of altitude error $h_e \geq 4.9$ m (16 ft). Of course, this hang-off error can be removed by means of an integrator in the altitude error channel. Because of bandwidth limitation, such trim corrections will be too slow for many maneuvers. Consequently, when such errors cannot be tolerated, even the relatively small transition as between A_1 and A_2 must be considered nonlinear for the purposes of generating trim controls. So, as usual, the practical concept of linearity is intimately related to accuracy requirements.

The trim problem is further complicated by the presence of redundant controls. Thus, as shown in figure 14, the total lift and drag coefficients required for steady flight at 65 knots along the -7.5° glide slope (point A_1) can be achieved by the trim condition $(\alpha,\nu,\delta_T,\delta_F) = (2.5,92,22,65)$. However, the same coefficients can be achieved by other combinations of controls. This redundancy is shown in figure 15, where point A_1 corresponds to the particular solution A_1 in figure 14. The question (the redundant control problem) is which combination $(\alpha,\nu,\delta_T,\delta_F)$ to use in any given situation.

The preceding discussion of the characteristics of the AWJSRA implies that careful attention must be given to the problem of trimming the aircraft. Present indications are that other aircraft types that use powered lift and

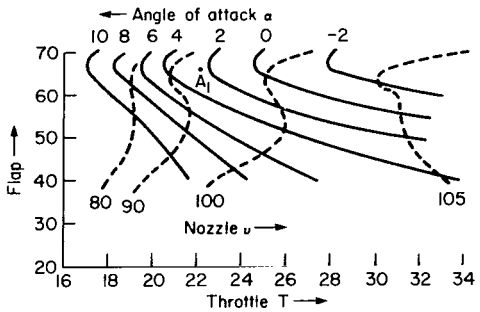

Figure 15.- Controls for one value of total force coefficient.

undergo rapid changes in configuration are similarly nonlinear and have redundant controls. Hence the following decision is made concerning the structure of the automatic flight-control system.

Decision 4: The control logic contains a section in which the control redundancy is resolved and trim controls are generated continuously. This section of the control logic is referred to as the trimmap.

The Trimmap

To solve the trim problem, one must, in effect, reverse some of the information flow shown in figure 9. Thus, given the relative velocity v_s and density ρ, and the commanded (trim) total force vector f_{sc} and moment vector M_{ac}, the problem is to find the required trim controls u_c. From equation (20), it follows that

$$C_{sc} = (QS_w)^{-1} f_{sc} \tag{26}$$

Since drag is defined as the force component along $-v_s$, and lift is defined as the total force perpendicular to v_s,

$$\left.\begin{aligned} C_{Dc} &= -u_s^T C_{sc} \\ C_{Lc} &= (C_{sc}^T C_{sc} - C_{Dc}^2)^{1/2} \end{aligned}\right\} \tag{27}$$

where u_s is defined by equation (6).

Two cases arise in the computation of the commanded side-force angle σ_c (see fig. 8), according to whether or not the commanded (trim) attitude of the aircraft A_{cs}^* is completely defined outside the trimmap.

If A_{cs}^* is completely defined, then the commanded angle of attack α_c and side-slip angle β_c are defined because the relative velocity vector v_s is not subject to control within trimmap; when in trim, $v_a = A_{cs}^* v_s$ and α and β are defined by equation (10). Consequently, the wind-tunnel coordinates (see fig. 7) of the total aerodynamic and propulsive force vector coefficient required for trim are given by

$$C_{wtc} = E_3(\beta_c) E_2^T(\alpha_c) A_{cs}^* C_{sc} \tag{28}$$

while equation (21) implies that

$$\sigma_c = \arctan[C_{wtc}(2),\ -C_{wtc}(3)] \tag{29}$$

so the problem is reduced to that of partially inverting the basic data of equations (19) and (25):

$$\left.\begin{aligned} C_D(\alpha,\beta,u;\eta) - C_{Dc} &= 0 \\ C_L(\alpha,\beta,u;\eta) - C_{Lc} &= 0 \\ \sigma(\alpha,\beta,u;\eta) - \sigma_c &= 0 \\ C_M(\alpha,\beta,u;\eta) - C_{Mac} &= 0 \end{aligned}\right\} \tag{30}$$

If A^*_{cs} is incompletely defined in that the trimmap is free to select the commanded angle of attack, then this angle and the controls must be chosen to satisfy equation (27) with constraints (30), which define the side-force angle σ_c. Then the commanded attitude can be defined according to equation (12), namely,

$$A^*_{cs} = E_2(\alpha_c)E_3^T(\beta_c)E_1(\phi_v)E_2(\gamma_v)E_3(\psi_v) \tag{31}$$

where

$$\phi_v = -\sigma_c + \arctan[C_{vc}(2),\ -C_{vc}(3)] \tag{32}$$

and (see fig. 7)

$$C_{vc} = E_2(\gamma_v)E_3(\psi_v)C_{sc} \tag{33}$$

The commanded attitude can also be defined without the explicit use of the angles (ϕ_v,γ_v,ψ_v) as follows. The unit vector u^p_s along the lift vector is given by

$$u^p_s = (C_{sc} + C_{Dc}u_s)/C_{Lc} \tag{34}$$

where C_{Dc} and C_{Lc} are defined by equation (27). Let the matrix U_{us} be the rotation defined by

$$U_{us} = [u_s,\ -S(u_s)u^p_s,\ -u^p_s] \tag{35}$$

where S is the vector cross-product operator defined by equation (12). The rotation U_{us} takes the axes that are initially aligned with the runway (inertial) axes into the attitude in which the relative velocity is along δ_1 and the lift vector is along $-\delta_3$. Hence the trim attitude is also given by

$$A^*_{cs} = E_2(\alpha_c)E_3^T(\beta_c)E_1(\sigma_c)U_{us} \tag{36}$$

The main flow of information in the automatic trim logic when the commanded attitude is incompletely defined is shown in figure 16. The primary inputs are the input translational acceleration $\dot{V}_{sI}$ and the input angular acceleration $\dot{\omega}_{aI}$. The output is the control, u, and the required trim attitude, A^*_{cs}. The solution of equations (30) (called the trimmap) is the core of the automatic trim logic. Within the trimmap, control redundancy is resolved and control strategy is modified in case of component failures. The trimmap provides a natural setting for monitoring the proximity of the aircraft to its performance limits and for protecting the aircraft from exceeding its design limits, that is envelope limiting. Furthermore, the primary purpose of the automatic trim logic is to provide a priori open-loop information to the overall automatic flight-control system and thereby relieve the perturbation controller whose feedback is intended to control the uncertainties of the process as well as relatively insignificant details that are known but ignored in the construction of the trimmap. Thus, it is also within trimmap that the major tradeoff between complexity and computer capacity on the one hand and accuracy of performance on the other takes place.

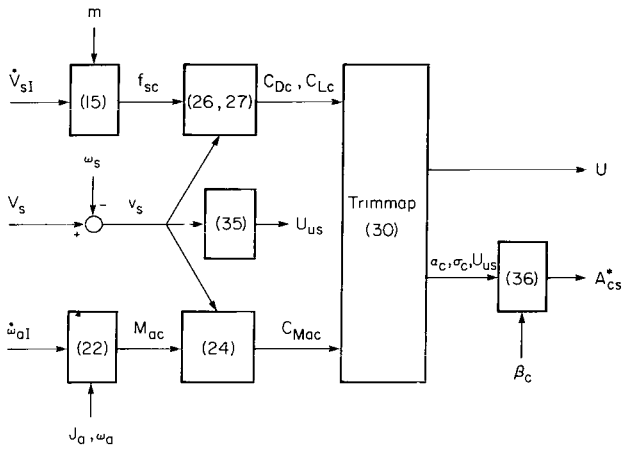

Figure 16.- Main information flow in automatic trim logic.

The perturbation controller is discussed in the next section. However, note that the relative velocity vector v_s is used in the trim logic. Since wind contributes significantly to the relative velocity, estimates of the wind must generally be computed. For this reason, the following decision regarding the structure of the automatic flight-control system is made.

Decision 5: The control logic includes a wind filter that estimates the inertial coordinates, w_s, of the wind vector. (The wind filter is discussed further later in the report.)

Perturbation Controller

The perturbation controller provides closed-loop, feedback control over details of the physical process not accounted for in the open-loop, feedforward, trim control either because they are not known a priori or because they have been purposely ignored to simplify the open-loop control. For the purposes of discussion, let the system state equation be

$$\dot{x} = f(x,u) \tag{37}$$

where x and u are the state and control, respectively, of appropriate dimension and, in addition, the control is restricted to a set U that may depend on the state. A trajectory $[x_o(t),\ t \in T]$ is flyable if, for all t in T, there is a control $u_o(t)$ such that

$$\dot{x}_o(t) = f[x_o(t),\ u_o(t)] \tag{38}$$

The trim problem (as discussed previously) is to find a control u_o that satisfies equation (38), given that the trim (nominal) trajectory x_o is flyable. The solution will be an inverse of the state equation (37), namely, a function (g,F), which we call the trimmap, so that for all $(\dot{x},x)$ in F,

$$f[x,g(\dot{x},x)] = \dot{x} \tag{39}$$

The corresponding trim control is given by

$$u_o = g(\dot{x}_o,x_o) \tag{40}$$

Usually, trim refers to cases with constant u_o. Here the concept is generalized to include open-loop controls that vary with time. As noted previously, when controls are redundant, the state equation (37) alone does not suffice to define the trimmap (g,F), and additional conditions must be introduced to resolve the redundancy.

The trim problem may be difficult to solve, but, evidently, its solution to the required accuracy is the essential first step in any design of automatic flight-control systems. The next step usually is to design feedback control systems based on perturbation models. Thus, given a flyable trajectory $(\dot{x}_o,x_o)$ trimmed by u_o according to equation (40), the linear model (41) is obtained for the perturbations $\delta x = x - x_o$ and $\delta u = u - u_o$:

$$\delta\dot{x} = \left(\frac{\partial f}{\partial x}\right)_o \delta x + \left(\frac{\partial f}{\partial u}\right)_o \delta u \tag{41}$$

where the partial derivatives are evaluated along the nominal trajectory. Then the application of the methods of linear control theory (ref. 5) yields the perturbation control law

$$\delta u = K_o \delta x \tag{42}$$

Since the coefficients in equation (41) depend on the nominal trajectory, the process must be repeated for a sufficiently large number N of nominal trajectories $(\dot{x}_o,x_o)$ in F until the flight envelope F is covered adequately. The result is a scheduled gain matrix $K(\dot{x}_o,x_o)$ and the complete control law is given by

$$u = g(\dot{x}_o,x_o) + K(\dot{x}_o,x_o)(x - x_o) \tag{43}$$

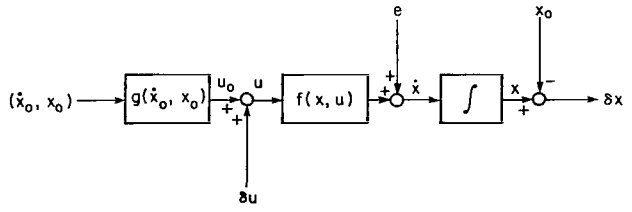

Figure 17.- Selected structure in conventional design.

The structure of the control system selected in the conventional perturbation controller design is shown in figure 17. The disturbance is represented by e.

The many advantages of the methods of quadratic optimization of linear systems are well publicized (ref. 5). Indeed, these methods are very powerful. But when the state equation (37) is highly nonlinear, the procedure for choosing the proper set $\{(\dot{x}_{oi}, x_{oi})\}_N$ of nominal trajectories to adequately cover the flight envelope F with perturbation models so as to apply these methods to each of them is, at present, rather unclear. Then there is the problem of how to obtain envelope limiting. The perturbation control δu (see fig. 17) may, in response to a disturbance, force the aircraft outside its design limits even though the nominal control u_o is maintained by the trimmap well within these limits. If envelope limiting is achieved by limits δU on δu, then questions concerning the stability of the resulting nonlinear perturbation controller must be resolved for each of the N perturbation models. Since these limits on u are likely to depend on $(\dot{x}_o, x_o)$, $\delta U(\dot{x}_o, x_o)$ must be stored in the control logic in addition to the gain matrix $K(\dot{x}_o, x_o)$ and the trimmap $g(\dot{x}_o, x_o)$. If N discrete cases of these variables are stored, the dynamics of switching from one case to the next as the aircraft state moves through their domains of validity must be designed. For example, hysteresis may have to be introduced to prevent jitter when the aircraft is required to fly near the boundary separating these regions. Switching dynamics further increase the storage and computation requirements of the flight computer. Lastly, there is a plethora of problems associated with reliability. Typically, does the system remain stable when a column or row of the gain matrix K is lost? — which corresponds to the loss of a sensor or a control, respectively. Such questions concerning the structure of the feedback are, as yet, difficult within the framework of quadratic optimization. In this respect, the older classical design techniques based on sequential loop closures that result in a nesting (hierarchy) of subsystems with decreasing bandwidth are more effective for designing fail-safe systems.

Because of these considerations, the following decisions are made concerning the formal structure of the automatic flight-control system.

Decision 6: The feedback is closed through the automatic trim logic.

Decision 7: The structure of the control logic is hierarchical.

The information flow implied by decision 6 is shown in figure 18. The feedback is through perturbation $\delta \dot{x}_o$ in the trim condition $\dot{x}_o$. Suppose that, initially, $x = x_o$. In the absence of any modeling errors, the control

$$u = g(\dot{x}_o, x) \tag{44}$$

will maintain $x = x_o$. The tracking will be perfect even if, at some point in time, $\dot{x}_o$ is perturbed to $\dot{x}_o + \delta\dot{x}_o$, provided that $(\dot{x}_o + \delta\dot{x}_o, x)$ is in F. The corresponding control is

$$u = g(\dot{x}_o + \delta\dot{x}_o, x) \qquad (45)$$

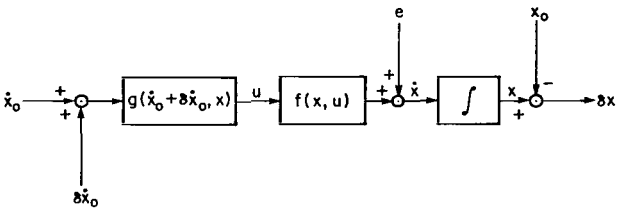

Figure 18.- Structure of proposed perturbation controller.

Now suppose that initially $x - x_o \neq 0$, but that the error can be removed by means of a flyable trajectory. Then there is an $\dot{x}_o + \delta\dot{x}_o$ that will take x into x_o by means of the control law given by equation (45). That is, the feedback for controlling the process uncertainties can be closed through the automatic trim logic as in figure 18 rather than after the trim logic as in figure 17. One immediate consequence is that envelope limiting is done within the trimmap. The other consequence is that, for any admissible $\delta\dot{x}_o$, the perturbation model is given anywhere inside F by

$$\delta\dot{x} = \delta\dot{x}_o + e \qquad (46)$$

where the magnitude of the error e depends on the accuracy of the automatic trim logic. Thus the emphasis is shifted from the N perturbation models required to cover F to the construction of flyable perturbations in the commanded trajectories. The latter task is considerably simplified by decision 7.

Consider the block diagram in figure 19, which represents the automatic flight-control system as viewed from one level in the hierarchy, namely, that

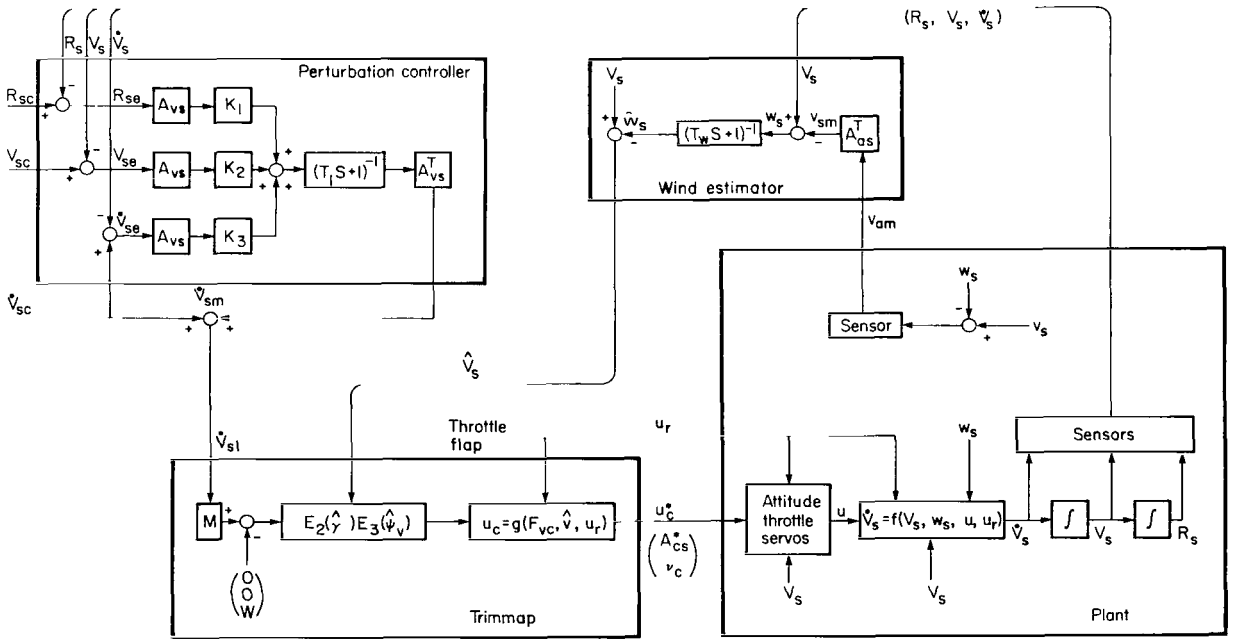

Figure 19.- Acceleration controller for the AWJSRA.

of the acceleration controller. The function of the acceleration controller is to accept commands from the command generator, which is one level higher, and transform them into commands to the flap, throttle, and nozzle servos, as well as to the attitude control system, all of which are one level lower. At the level of the acceleration controller, the servo systems are represented by relatively simple, possibly linear and low-order, input-output relations, which are treated as specifications to be met in the design of these subsystems. Of course, the subsystems may be quite complicated internally. For example, the attitude control system may have its own automatic trim logic and perturbation controller and may rely on simple input-output relations that describe the control surface servos, which are another step lower in the hierarchy.

The major blocks of the acceleration controller are the trimmap, wind filter, and compensator. The inertial coordinates $\dot{V}_{sI}$ of the input acceleration vector are transformed by the trimmap (fig. 16) into commanded flap, throttle, nozzle, and attitude.

The wind filter computes smoothed inertial coordinates $\hat{w}_s$ of aircraft velocity relative to the air mass from body-mounted air velocity v_{am} sensors and from the inertial velocity V_s and attitude A_{as} of the aircraft. Note that only the inertial coordinates of wind are filtered, while V_s is unaffected. Hence, in the absence of wind and, of course, sensor errors, $\hat{v}_s = V_s$.

The input-output relation, $\dot{V}_{sI} \rightarrow \dot{V}_s$, where the $\dot{V}_s$ terms are the inertial coordinates of aircraft acceleration vector, is given by (see eq. (46)),

$$\dot{V}_s = \dot{V}_{sI} + e \tag{47}$$

where e depends on the inaccuracies of the trimmap and the wind filter, the presence of unsteady aerodynamics such as $\dot{\alpha}$ effects, and on attitude and other subsystem dynamics. The purpose of the perturbation controller is to close the loop around such effects and thereby reduce e to a tolerable level. Inertial coordinates of position, velocity, and acceleration errors are transformed into approximately longitudinal, lateral, and normal errors by means of the direction cosine matrix A_{vs} computed from the commanded inertial velocity V_{sc}; the errors are weighted by constant gain matrices K_1, K_2, and K_3 commensurate with the acceleration capacities of the aircraft in these directions. The result is filtered to ensure compatibility with the attitude control system and other subsystem dynamics. The corrective acceleration is transformed back into inertial space and added to command $\dot{V}_{sc}$ to give input $\dot{V}_{sI}$. In this way, feedback is closed around the process uncertainties, e, so that

$$\dot{V}_s = \dot{V}_{sc} \tag{48}$$

is sufficiently accurate if the acceleration $\dot{V}_{sc}$ commanded by the command generator is admissible, namely, if $(V_{sc}, \dot{V}_{sc})$ is flyable and the bandwidth of $\dot{V}_{sc}$ is suitably restricted. Coriolis terms due to the time rate of change of A_{vc} may be included in the perturbation controller if necessary using the techniques of the next section.

Angular Acceleration Controller

The discussion thus far has been concerned with controlling the motion of aircraft's center of mass. The concepts that led to the structure of the (translational) acceleration controller shown in figure 19 are also applied to formulate the structure of the angular acceleration controller. The function of the angular acceleration controller is to accept commands from the attitude command generator and transform them into commands to the wheel, elevator, and rudder servos. The structure is again hierarchical. The attitude command generator, one step above the angular acceleration controller, accepts attitude requests from the translational control system and, based on simple input-output representation, generates rotational trajectories $[A_{cs}(t), \omega_c(t), \dot{\omega}_c(t)]$ as input to the angular acceleration controller. The control surface servos, one step below the angular acceleration controller, are represented by relatively simple, input-output relations.

The structure of the angular acceleration controller is shown in figure 20. The major blocks are the moment trimmap, wind estimator, and attitude perturbation controller. The body coordinates $\dot{\omega}_{aI}$ of the input angular acceleration vector are transformed by the moment trimmap into commanded wheel $\delta\omega_c$, elevator δe_c, and rudder δ_{rc}.

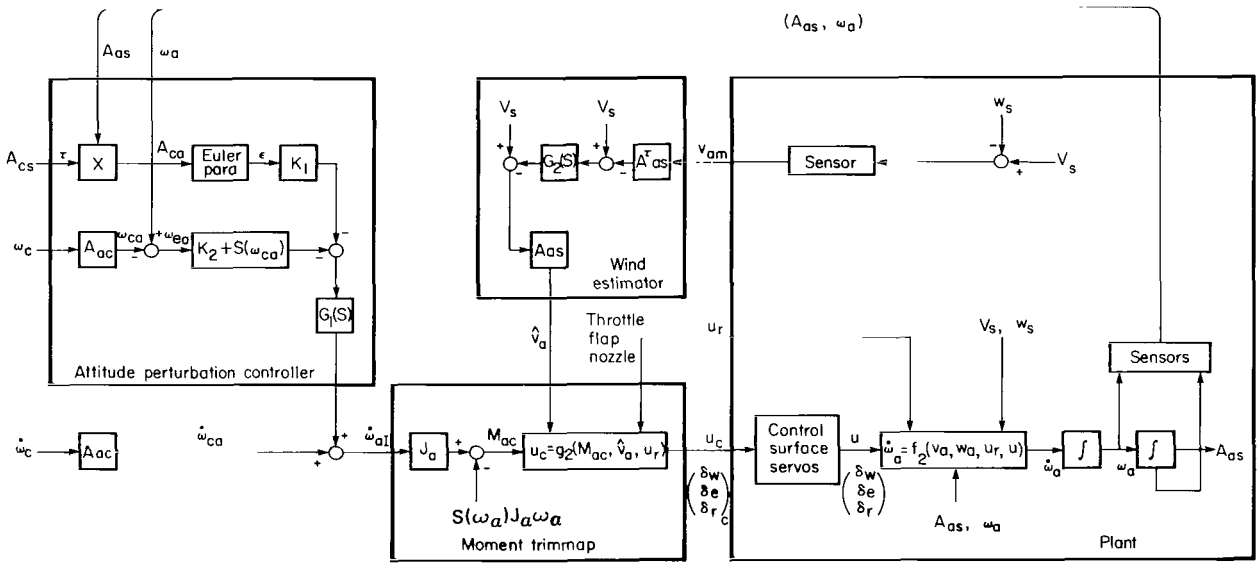

Figure 20.- Structure of the angular acceleration controller for the AWJSRA.

The wind estimator provides estimates of the body coordinates $\hat{v}_a$ of aircraft velocity relative to the air mass, which are needed in the moment trimmap calculations. The structure is very similar to that of the wind estimator in the translational control system. There may be differences in detail because of different bandwidth requirements.

The input-output relation, $\dot{\omega}_{ai} \rightarrow \dot{\omega}_a$, is given by

$$\dot{\omega}_a = \dot{\omega}_{ai} + e \tag{49}$$

where e depends on the inaccuracies of the moment trimmap and the wind estimator, the presence of unsteady aerodynamics such as $\dot{\alpha}$ effects and wind shear across the aircraft, and on the dynamics of control surface servos. The purpose of the attitude perturbation controller is to close the loop around such effects and thereby reduce the error e to a tolerable level. Following reference 4, attitude error is defined by the direction cosine matrix

$$A_{ac} = A_{as}A_{cs}^T \tag{50}$$

that represents the aircraft attitude relative to the commanded attitude. The time derivative is

$$\dot{A}_{ac} = \dot{A}_{as}A_{cs}^T + A_{as}\dot{A}_{cs}^T$$

But (see eq. (14)),

$$\dot{A}_{as} = S(\omega_a)A_{as}$$

and

$$\dot{A}_{cs} = S(\omega_c)A_{cs}$$

where ω_a represents (in body axes) the aircraft angular velocity relative to the runway, and ω_c represents (in the commanded body axes) the commanded angular velocity relative to the runway, Hence

$$\begin{aligned}
\dot{A}_{ac} &= S(\omega_a)A_{ac} - A_{ac}S(\omega_c) \\
&= S(\omega_a)A_{ac} - A_{ac}S(\omega_c)A_{ac}^T A_{ac} \\
&= S(\omega_a)A_{ac} - S(A_{ac}\omega_c)A_{ac} \\
&= S(\omega_a - A_{ac}\omega_c)A_{ac}
\end{aligned}$$

or, equivalently,

$$\dot{A}_{ac} = S(\omega_{ea})A_{ac} \tag{51}$$

where the body coordinates of angular velocity error are given by

$$\omega_{ea} = \omega_a - A_{ac}\omega_c \tag{52}$$

Therefore, the time derivative is

$$\dot{\omega}_{ea} = \dot{\omega}_a - S(\omega_{ea})A_{ac}\omega_c - A_{ac}\dot{\omega}_c$$

$$= \dot{\omega}_a + S(\omega_{ca})\omega_{ea} - A_{ac}\dot{\omega}_c$$

where $\omega_{ca} = A_{ac}\omega_c$ represents (in the body axes) the commanded angular velocity. The identity $S(x)y = -S(y)x$ was used in the last step above. Thus the body coordinates of angular acceleration are expressed in terms of the command and perturbations as

$$\dot{\omega}_a = A_{ac}\dot{\omega}_c - S(\omega_{ca})\omega_{ea} + \dot{\omega}_{ea} \tag{53}$$

Note that, since no small signal approximations are used to derive equation (53), it is universally valid.

Equation (53) can be interpreted as defining the required angular acceleration $\dot{\omega}_{aI}$ of the aircraft (which is the input to the moment trimmap), so that the command is executed with perturbation $(A_{ac},\omega_{ea},\dot{\omega}_{ea})$. An equation connecting $\dot{\omega}_{ea}$ to (A_{ac},ω_{ea}) closes the loop around the perturbations. Thus the remaining problem is to synthesize a control law $h = h(A_{ac},\omega_{ea})$ so that the system

$$\begin{aligned} \dot{A}_{ac} &= S(\omega_{ea})A_{ac} \\ \dot{\omega}_{ea} &= h \end{aligned} \tag{54}$$

has an acceptable relaxation transient response, $[A_{ac}(0),\omega_{ea}(0)] \rightarrow (I,0)$. This problem is treated in some detail in references 4 and 6. For example, the attitude error is defined by

$$\varepsilon = 0.5 \begin{pmatrix} a_{23} - a_{32} \\ a_{31} - a_{13} \\ a_{12} - a_{21} \end{pmatrix}$$

where $(a_{ij}) = A_{ac}$. According to Euler's theorem on rotations, every attitude can be attained with a single rotation. Let ϕ be the angle of A_{ac}, and let e be the unit vector along the axis of A_{ac}. It can be shown that $\varepsilon = (\sin\phi)e$. Thus, for small attitude errors ($\phi \leq 0.5$ radian), ε gives both the magnitude and direction of attitude error. In addition, for small perturbations,

$$\dot{\varepsilon} = \omega_{ea}$$

is a good approximation to the kinematic equation, and the state equation (54) becomes

$$\dot{\varepsilon} = \omega_{ea}$$

$$\dot{\omega}_{ea} = h$$

There are many techniques for synthesizing the control law h. A simple example is

$$h = - K_1\varepsilon - K_2\omega_{ea} \tag{55}$$

where the constant gain matrices K_1 and K_2 are selected to provide the required bandwidth and damping in each axis.

With the control law (55), the input to the moment trimmap becomes

$$\dot{\omega}_{aI} = A_{ac}\dot{\omega}_c - \{K_1\varepsilon + [K_2 + S(\omega_{ca})]\omega_{ea}\} \tag{56}$$

(shown schematically in fig. 20). The dynamic element $G_1(s)$ is included in the attitude perturbation controller to provide high-frequency cutoff. Thus, a feedback is closed around the process uncertainties, e, in equation (49) so that

$$\dot{\omega}_a = \dot{\omega}_c \tag{57}$$

is sufficiently accurate if the angular acceleration command, $\dot{\omega}_c$, commanded by the attitude command generator is admissible, namely, if $(A_{cs},\omega_c,\dot{\omega}_c)$ is flyable and if the bandwidth of $\dot{\omega}_c$ is suitably restricted.

Now, consider the translation perturbation controller discussed at the end of the preceding section. The Coriolis effects may be included as follows. Let the matrix A define an axis system with respect to inertial space, and let $R_e = A(R_{sc} - R_s)$ and $V_e = A(V_{sc} - V_s)$ be the position and velocity errors, respectively. Then $\dot{A} = S(\omega)A$, where ω is the angular velocity of A, and

$$\dot{R}_e = S(\omega)R_e + V_e$$

$$\ddot{R}_e = S(\dot{\omega})R_e + S(\omega)[S(\omega)R_e + V_e] + S(\omega)V_e + A(\dot{V}_{sc} - \dot{V}_s)$$

Hence,

$$\dot{V}_s = \dot{V}_{sc} + A^T[S(\dot{\omega})R_e + S^2(\omega)R_e + 2S(\omega)V_e - \ddot{R}_e]$$

The designer is free to choose A and $\ddot{R}_e$. For example, let the error relax according to the linear law,

$$\ddot{R}_e = -K_1R_e - K_2\dot{R}_e$$

Then the input to the trimmap is given by

$$\dot{V}_{sI} = \dot{V}_{sc} + A^T\{[S(\dot{\omega}) + S^2(\omega) + K_2S(\omega) + K_1]R_e + [2S(\omega) + K_2]V_e\}$$

In particular, if $A = A_{vs}$, which aligns the first axis with the commanded velocity, V_{sc}, and maintains the second axis horizontal, then

$$\omega = \omega_v = -(A_{vs} + k\delta_1\delta_3^T)S(V_{sc})\dot{V}_{sc}/V_c^2$$

where

$$k = \frac{\delta_3^T u_{sc}}{1 - (\delta_3^T u_{sc})^2}, \qquad u_{sc} = \frac{V_{sc}}{V_c}, \qquad V_c = (V_{sc}^T V_{sc})^{-1/2}$$

The results of simulation tests suggest that all significant coriolis effects are accounted for by the approximation in which $k = 0$ and the gains in figure 19 are replaced as follows,

$$K_1 \leftarrow S^2(\omega_v) + K_2S(\omega_v) + K_1$$

$$K_2 \leftarrow 2S(\omega_v) + K_2$$

and K_3 is unchanged.

Trajectory Command Generator

The last two major blocks of the proposed structure of automatic flight-control systems are the trajectory command generator and the attitude command generator. Their function is to provide only admissible commands to the corresponding acceleration controllers. In this section, only the trajectory command generator is discussed. Since, within the scope of this report, the two generators may be considered to be very similar, the discussion applies also to the attitude command generator.

In the hierarchy of control logic, the command generator is one level above the acceleration controller and one level below the generalized air traffic control (which includes the pilot). Sufficiently smooth commands can be passed unmodified to the acceleration controller. However, in general, discontinuities will be present: the air traffic control may request a discontinuous change in trajectory; the pilot may switch to a different control mode; the set of active sensors may change; or a strong disturbance due to wind or a partial failure may force the aircraft too far from the commanded trajectory to be brought back by the perturbation controller. In such cases, the command generator must generate an acceptable transition (flare) trajectory that returns the aircraft on target. The transition may be generated by means of a dynamical system as shown in figure 21.

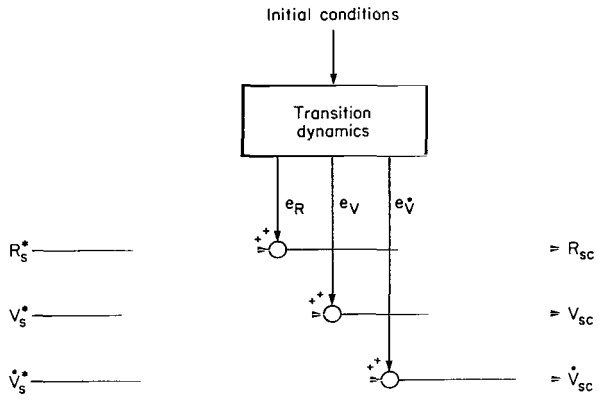

Figure 21.- Generation of transition (flare) trajectory.

The output of the command generator is given by

$$\begin{pmatrix} R_{sc} \\ V_{sc} \\ \dot{V}_{sc} \end{pmatrix} = \begin{pmatrix} R_s^* \\ V_s^* \\ \dot{V}_s^* \end{pmatrix} + \begin{pmatrix} e_R \\ e_V \\ e_{\dot{V}} \end{pmatrix} \tag{58}$$

where the quantities $(\ )^*$ are the ATC command (see eq. (1)), and e_R, e_V, and $e_{\dot{V}}$ are the modifications of that command in position, velocity, and acceleration.

Let the differential equation of the transition dynamics be

$$\dot{e} = h(e) \tag{59}$$

with an output map

$$\begin{pmatrix} e_R \\ e_V \\ e_{\dot{V}} \end{pmatrix} = H(e) \tag{60}$$

If equation (59) is asymptotically stable and $H(0) = 0$, the output of the command generator will approach the ATC command with time. To have continuity in commanded position, velocity, and acceleration, the dimension of e must be at least 9, that is, 3 for each axis. If initial conditions are chosen so that

$$\begin{pmatrix} e_R(0) \\ e_V(0) \\ e_{\dot{V}}(0) \end{pmatrix} = \begin{pmatrix} R_s(0) - R_s^*(0) \\ V_s(0) - V_s^*(0) \\ \dot{V}_s(0) \quad \dot{V}_s^*(0) \end{pmatrix} \tag{61}$$

then, at the initiation of the transition, the command coincides with the actual position, velocity, and acceleration of the aircraft.

The detailed shape of the transition is controlled by means of the function $h(e)$ in the state equation (59). Generally, the state space will consist of at least two regions, one of which includes the origin $e = 0$. In this region, the function $h(e)$ may be linear. Thus, for example, let the small transitions be generated by three uncoupled, linear systems with constant coefficients,

$$\dot{e}_i = F_i e_i \tag{62}$$

where, for each $i = 1,2,3$, the dimension of e_i is 3 and the dimension of the constant matrices F_i is 3×3. If the initial conditions are defined by the rows of the matrix

$$e(0) = A_{vc}[e_R(0), e_V(0), e_{\dot{V}}(0)] \tag{63}$$

and the output map is defined by

$$[e_R(t), e_V(t), e_{\dot{V}}(t)] = A_{vc}^T e(t) \tag{64}$$

then the transition dynamics will be approximately invariant with respect to the commanded velocity axes given by the matrix A_{vc}. Since the acceleration controller tracks the output of the command generator with small error, equation (62) represents approximately the transition dynamics with respect to the longitudinal ($i = 1$), lateral ($i = 2$), and normal ($i = 3$) axes of the aircraft, respectively. The bandwidth of the transition can be made compatible with the restrictions of acceleration controller by a proper choice of matrices F_i.

Outside a neighborhood of $e = 0$, the function $h(e)$ must be modified; otherwise, the magnitude restrictions of the acceleration controller will be violated. In this region of the state space of e, the design of $h(e)$ may be based on such considerations as the optimization of transit time or transit energy with hard constraints on e.

In effect, trajectory tracking errors have been sorted into three levels. Small errors are corrected by the perturbation controller without reinitializing the command generator. Medium errors are corrected by means of the command generator with linear transition dynamics. Large errors are corrected by means of the command generator with nonlinear dynamics.

The total output of the command generator is given by equation (58). The generalized ATC command $(R_S^*, V_S^*, \dot{V}_S^*)^T$, when not provided explicitly as a function of time by ATC, must be generated onboard from a set of trajectory parameters that are either signaled by ATC or selected by the pilot.

Finally, the command generator must contain a subblock within which autopilot modes can be defined for the control logic. The essential function of the mode variable is to specify which parameters of the commanded trajectory are to be tracked. A very simple example is given in table 2.

TABLE 2.- EXAMPLE OF A MODE VARIABLE

Trajectory parameter to be tracked	Axis		
	Longitudinal	Lateral	Vertical
Acceleration	0	0	0
Velocity	1	1	1
Position	2	2	2

The mode variable M in this case is three-dimensional. Each coordinate can take one of three values. Thus, there are 27 possible modes: M = (2,2,2) specifies position tracking in all three axes; M = (0,1,2) specifies the tracking of longitudinal acceleration, lateral velocity, and vertical position; and M = (1,1,1) represents velocity vector tracking mode, etc. Of course, other definitions of the mode variable are possible and are being investigated. Some of the commonly used modes can be included within the proposed structure by simply changing the set of active sensors. For example, if compass heading and barometric altitude are to be tracked instead of inertial heading and altitude, then compass and baro altimeter should be used for feedback instead of, say, MLS. Other modes, such as when the automatic flight-control system is allowed only limited authority and must interact with the pilot in the loop may be more difficult to include within the proposed structure, but present indications are that such inclusions are possible. For the present purposes, however, it is sufficient to note that the automatic control logic must include a mode definition subblock.

The proposed structure of the command generator is outlined in figure 22.

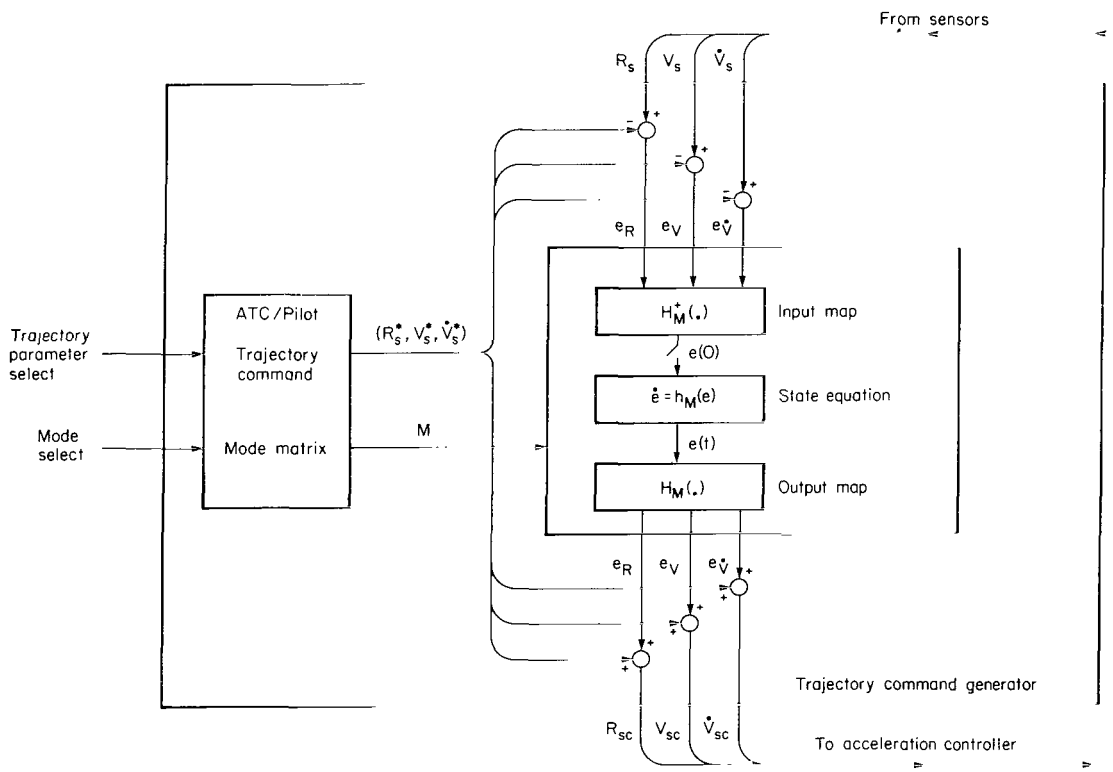

Figure 22.- Structure of the trajectory command generator.

PROPOSED STRUCTURE OF AUTOMATIC FLIGHT-CONTROL SYSTEM

The overall logical structure of the automatic flight-control system developed here is outlined in figure 23. The structure consists of five major subsystems, namely, the trimmap, wind filter, attitude and throttle control systems, perturbation controller, and command generator.

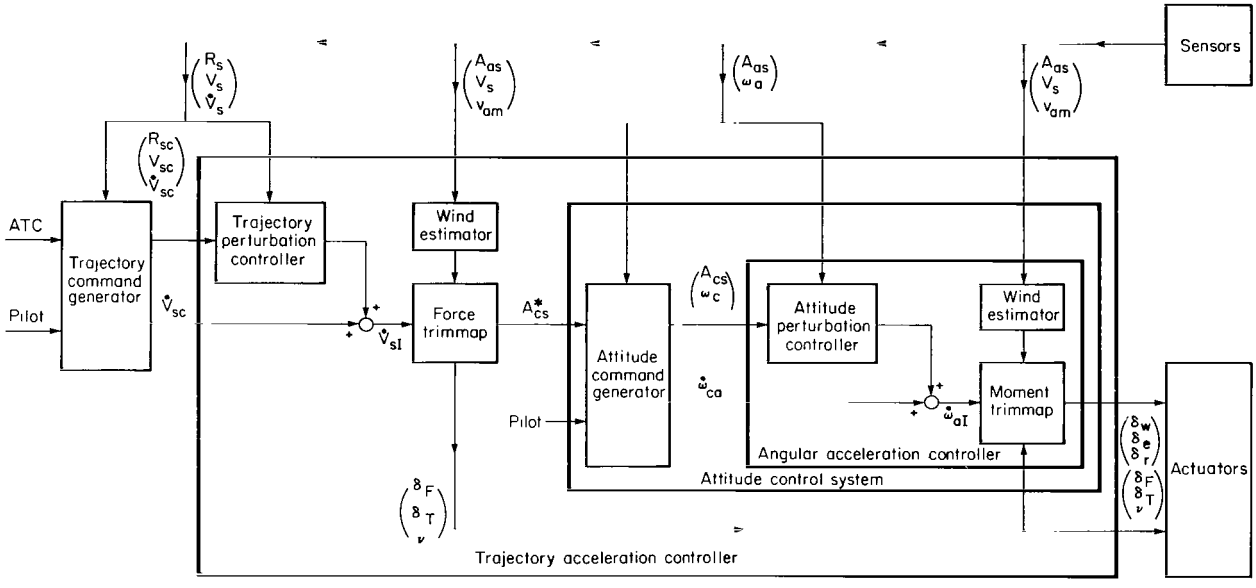

Figure 23.- Proposed structure of the automatic flight-control system for the AWJSRA.

The decision to include a trimmap is motivated by the need to provide automatic envelope limiting and by the impracticality of overcoming the highly nonlinear characteristics of the aircraft by means of high-gain feedback. In the trimmap, a priori information concerning the aircraft characteristics is used to generate open-loop control commands that trim the aircraft to a given acceleration vector.

The decision to include a wind filter is dictated by the fact that aerodynamic forces and moments are functions of the aircraft velocity relative to the air mass.

Considerations of reliability and simplicity motivated the decision to impose a hierarchy on the control logic. The six degrees of freedom of the rigid aircraft are partitioned into a three-dimensional translation system and a three-dimensional rotational system. The function of the attitude control system is to execute the attitude commands provided by the (translation) trimmap. The bandwidth of the attitude control system is an order of magnitude higher than the bandwidth of the translation control system.

Process uncertainties are controlled by means of a perturbation controller which closes the loop around the trimmap, wind filter, and attitude and throttle control systems. The design and implementation of the perturbation controller are drastically simplified by the decision to close the feedback through the trimmap.

The subsystem composed of the perturbation controller, trimmap, attitude and throttle control system, and wind filter is an acceleration controller. Its input-output relation between the commanded acceleration $\dot{V}_{sc}$ and actual aircraft acceleration $\dot{V}_s$ is approximately an identity everywhere on the flight envelope for suitably restricted acceleration commands. The function of the command generator is to give only admissible commands to the acceleration controller and to provide the interface between the control logic and the air traffic control or the pilot.

As stated in the introduction, the purpose of the present report is not to present a complete design of an automatic flight control system, but, rather, to outline a structure of such systems. The discussion in the report leads to the structure composed of five major subsystems which are interconnected as indicated in figure 23. Some of the details within these subsystems discussed in the report are intended primarily to further clarify the purpose of each subsystem rather than as final designs. Indeed, the detailed structure of each of the five subsystems is currently being developed and the results will be reported in forthcoming publications. However, the feasibility of the proposed structure has been tested by application to a simulation of the unmodified DHC-C8A and the Augmentor Wing Jet STOL Research Aircraft. The proposed logical structure has been shown to be feasible, and flight test evaluation will occur in the near future.

CONCLUSIONS

The proposed approach to the design of automatic flight control systems for advanced aircraft has several advantages, among which are the following.

The approach is applicable to a large class of aircraft.

The approach is nearly algorithmic.

The tracking accuracy enters as an independent variable which may be varied over a wide range.

There is an effective trade-off between tracking accuracy and flight computer requirements.

Because the approach leads to a hierarchical system, questions of reliability are tractable.

The approach has been shown to be feasible, and flight test evaluation will occur in the near future.

Ames Research Center
National Aeronautics and Space Administration
Moffett Field, Calif. 94035, February 12, 1975

REFERENCES

1. Erzberger, Heinz; and Lee, Homer Q.: Terminal-Area Guidance Algorithms for Automated Air-Traffic Control. NASA TN D-6773, 1972.

2. McGee, Leonard A.; Smith, Gerald L.; Hegarty, Daniel M.; Carson, Thomas M.; and Merrick, Robert B.: Flight Results from a Study of Aided Inertial Navigation Applied to Landing Operations. NASA TN D7302, 1973.

3. McRuer, Duane; Ashkenas, Irving; and Graham, Dunstan: Aircraft Dynamics and Automatic Control. Princeton University Press, 1973.

4. Meyer, George: On the Use of Euler's Theorem on Rotations for the Synthesis of Attitude Control Systems. NASA TN D-3643, 1966.

5. Anon.: Special Issue on Linear-Quadratic-Gaussian Estimation and Control Problem, IEEE Transactions on Automatic Control, vol. AC-16, no. 6, Dec. 1971, pp. 527-869.

6. Meyer, George: Design and Global Analysis of Spacecraft Attitude Control Systems. NASA TR R-361, 1971.

NASA-Langley, 1975 A-5710

"The aeronautical and space activities of the United States shall be conducted so as to contribute . . . to the expansion of human knowledge of phenomena in the atmosphere and space. The Administration shall provide for the widest practicable and appropriate dissemination of information concerning its activities and the results thereof."

—NATIONAL AERONAUTICS AND SPACE ACT OF 1958

NASA SCIENTIFIC AND TECHNICAL PUBLICATIONS

TECHNICAL REPORTS: Scientific and technical information considered important, complete, and a lasting contribution to existing knowledge.

TECHNICAL NOTES: Information less broad in scope but nevertheless of importance as a contribution to existing knowledge.

TECHNICAL MEMORANDUMS: Information receiving limited distribution because of preliminary data, security classification, or other reasons. Also includes conference proceedings with either limited or unlimited distribution.

CONTRACTOR REPORTS: Scientific and technical information generated under a NASA contract or grant and considered an important contribution to existing knowledge.

TECHNICAL TRANSLATIONS: Information published in a foreign language considered to merit NASA distribution in English.

SPECIAL PUBLICATIONS: Information derived from or of value to NASA activities. Publications include final reports of major projects, monographs, data compilations, handbooks, sourcebooks, and special bibliographies.

TECHNOLOGY UTILIZATION PUBLICATIONS: Information on technology used by NASA that may be of particular interest in commercial and other non-aerospace applications. Publications include Tech Briefs, Technology Utilization Reports and Technology Surveys.

Details on the availability of these publications may be obtained from:

SCIENTIFIC AND TECHNICAL INFORMATION OFFICE

NATIONAL AERONAUTICS AND SPACE ADMINISTRATION

Washington, D.C. 20546